Research Article

Journal of MASS SPECTROMETRY

Received: 2 February 2012 Revised: 20 March 2012 Accepted: 27 March 2012 Published online in Wiley Online Library

(wileyonlinelibrary.com) DOI 10.1002/jms.2999

Protomers: formation, separation and characterization via travelling wave ion mobility mass spectrometry

Priscila M. Lalli,[a] Bernardo A. Iglesias,[b] Henrique E. Toma,[b] Gilberto F. de Sa,[c,d] Romeu J. Daroda,[c] Juvenal C. Silva Filho,[d] Jan E. Szulejko,[e]* Koiti Araki[b]* and Marcos N. Eberlin[a]*

Travelling wave ion mobility mass spectrometry (TWIM-MS) with post-TWIM and pre-TWIM collision-induced dissociation (CID) experiments were used to form, separate and characterize protomers sampled directly from solutions or generated in the gas phase via CID. When in solution equilibria, these species were transferred to the gas phase via electrospray ionization, and then separated by TWIM-MS. CID performed after TWIM separation (post-TWIM) allowed the characterization of both protomers via structurally diagnostic fragments. Protonated aniline (1) sampled from solution was found to be constituted of a ca. 5:1 mixture of two gaseous protomers, that is, the N-protonated (1a) and ring protonated (1b) molecules, respectively. When dissociated, 1a nearly exclusively loses NH_3, whereas 1b displays a much diverse set of fragments. When formed via CID, varying populations of 1a and 1b were detected. Two co-existing protomers of two isomeric porphyrins were also separated and characterized via post-TWIM CID. A deprotonated porphyrin sampled from a basic methanolic solution was found to be constituted predominantly of the protomer arising from deprotonation at the carboxyl group, which dissociates promptly by CO_2 loss, but a CID-resistant protomer arising from deprotonation at a porphyrinic ring NH was also detected and characterized. The doubly deprotonated porphyrin was found to be constituted predominantly of a single protomer arising from deprotonation of two carboxyl groups. Copyright © 2012 John Wiley & Sons, Ltd.

Keywords: protomers, protonation site; aniline; pyridyl porphyrins; electrospray ionization; travelling wave ion mobility; mass spectrometry, gas phase acidity, gas phase basicity

INTRODUCTION

The determination of the intrinsically most favorable sites for protonation or deprotonation of molecules exhibiting multiple basic or acidic sites is a matter of great fundamental and practical relevance.[1] However, the analytical task involving the detection and characterization of ideally gaseous isomers resulting either from the addition (protomers) or removal of protons from different sites has been challenging. Several techniques have been employed for protomer characterization in the gas phase, but contrasting results have been reported for several molecules[1–8] including aniline, the most classical model for protonation site studies. Earlier calculations at the STO-3G level using isodesmic reactions have indicated preferable N-protonation as compared to ring protonation (preferably *para* to the amine group),[2] but with an energy difference of only 1–3 kcal mol^{-1}. Subsequent determinations of proton affinity suggested that some substituted-anilines were preferentially ring-protonated showing a contrasting behavior as compared with the parent aniline.[3] Collision-induced dissociation (CID) experiments gave similar results for *p*-alkylanilines, whereas N-alkylanilines were shown to be almost exclusively N-protonated.[4] In 1990, Karpas *et al.*[5] employing conventional ion mobility coupled to mass spectrometry (IM-MS) was able to separate two protomers of aniline which were tentatively assigned to the N- and ring-protonated isomers, but peak attribution could not be performed. Ion/molecule reactions have also been applied, indicating the co-existence of two gaseous protomers of aniline, the N-protonated isomer being kinetically favored.[6] More recently, Russo *et al.*[7] performed different levels of theoretical calculations showing that whereas the energy gap between N- and ring-protonated aniline at the

* *Correspondence to: Jan E. Szulejko, 26 Twyniago, Pontarddulais, Swansea, SA4 8HX, U.K. E-mail: jan.szulejko@btinternet.com*

* *Koiti Araki, University of São Paulo, Institute of Chemistry, Av. Prof. Lineu Prestes 748, CEP 05508–000, São Paulo, SP, Brazil. E-mail: koiaraki@iq.usp.br*

* *Marcos N. Eberlin, ThoMSon Mass Spectrometry Laboratory, Institute of Chemistry, University of Campinas, UNICAMP 13083–970, Campinas, SP, Brazil. E-mail: eberlin@iqm.unicamp.br*

a *ThoMSon Mass Spectrometry Laboratory, Institute of Chemistry, University of Campinas, UNICAMP 13083-970, Campinas, SP, Brazil*

b *University of São Paulo, Institute of Chemistry Av. Prof. Lineu Prestes 748, CEP 05508-000, São Paulo, SP, Brazil*

c *National Institute of Metrology, INMETRO, Division of Chemical Metrology 25250-020, Duque de Caxias, RJ, Brazil*

d *Federal University of Sergipe, Department of Chemistry, CEP 49500-000, Itabaiana, SE, Brazil*

e *26 Twyniago, Pontarddulais, Swansea, SA4 8HX, U.K.*

Journal of MASS SPECTROMETRY

para-position is very sensitive to the theoretical method employed, the results using the highest calculation levels (MP4 and G2(MP2)) were always consistent, suggesting that the protonation at the *para*-position of the aromatic ring is favored by only 0.5–0.7 kcal mol^{-1}, in accord with the CID experiments. Ion/molecule reactions of halobenzenes with ammonia, as well as electrospray ionization (ESI) were reported to produce dominantly N-protonated aniline, characterized by collision activation.[8] In all cases, therefore, the aniline N-atom and the C-atom at the *para*-position relative to the amine group are the most favorable protonation sites. However, despite the extensive work carried out with this prototype molecule, the exact proportion of aniline protomers sampled from solution or formed in the gas phase remains uncertain.

Ion mobility spectrometry (IMS) separates ions on the basis of their masses, charges and shapes (as usually measured by collision cross sections) while they travel through a drift gas under the influence of an electric field.[9] When combined to MS, IMS adds therefore shape as a new dimension of analysis in addition to *m/z* ratios, greatly increasing the range of analytical applications of MS.[10] IM-MS has therefore been employed to resolve several types of isomers,[11] in the characterization of complex mixtures, such as polymers[12] and crude oil,[13] in structural analyses of small molecules, supramolecular assemblies[14] and biomolecules.[15] Recently, travelling wave ion mobility (TWIM) has been coupled to MS and introduced as a new mode of ion propulsion (and separation) for TWIM-MS experiments.[16] Unlike conventional IMS, in which a low electric field is applied continuously to the IM cell, TWIM uses a continuous train of transient voltage pulses (travelling waves) to drift the ions through a very compact and effective IM cell (18.5 cm long). For structural elucidation, a unique and welcome feature of the commercial TWIM-MS setup is the possibility to perform either pre-TWIM or post-TWIM CID of mass selected ions. Recently, we have demonstrated the possibility of analyzing mixtures of ruthenated *meso*-phenyl(meta- and para-pyridyl) porphyrin isomers by TWIM-MS.[17] Herein, using four model molecules (Scheme 1), we have tested the ability of TWIM-MS to form, separate, quantitate and characterize protomers of aniline (**1**) and several porphyrins (**2–4**) using CO_2, a relatively massive and polarizable drift gas[18] in an attempt to enhance resolution.

EXPERIMENTAL

Travelling wave ion mobility experiments

TWIM-MS experiments were performed using a first generation Waters Synapt HDMS (high-definition mass spectrometer, Manchester, UK). This instrument, described in detail elsewhere,[16] has a hybrid quadrupole/ion mobility/orthogonal acceleration time-of-flight geometry. Acidic methanolic solutions of aniline (**1**), *meso*-tetra(4-pyridyl)porphyrin (**2**) and *meso*-tetra(3-pyridyl) porphyrin (**3**) were analysed separately via ESI in the positive ion mode, whereas a basic methanolic solution of *meso*-tetra (4-carboxyphenyl)porphyrin (**4**) was analyzed via ESI in the negative ion mode.

In our Synapt HDMS instrument, the TWIM entrance and exit apertures were reduced from 2-mm to 1-mm diameter to allow drift gas pressure to be efficiently increased over 1 mbar without any substantial detrimental effect on MS performance.

Typical ESI(±) source conditions were as follows: capillary voltage 3.0 kV or 2.5 kV (for positive and negative ion mode, respectively), sample cone 30 V, extraction cone 3.0 V, source temperature 100 °C, desolvation temperature 100 °C, desolvation flow rate 400 mL min^{-1} of N_2. In all experiments, the ions of interest were mass selected by the quadrupole prior to TWIM separation. The TWIM cell was operated at a pressure of 1.0 mbar of CO_2, with wave velocity and wave height adjusted for each species analyzed (Table 1) such that the ion drift times were centered in the drift time window. For MS experiments,

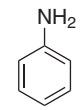

Aniline (1)

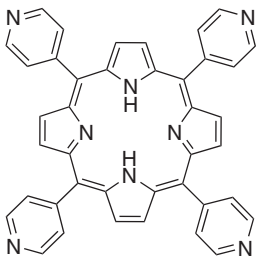

meso-tetra(4-pyridyl)porphyrin (2)

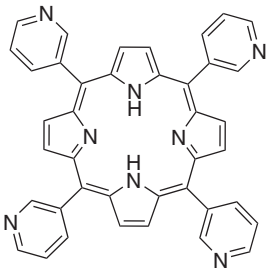

meso-tetra(3-pyridyl)porphyrin (3)

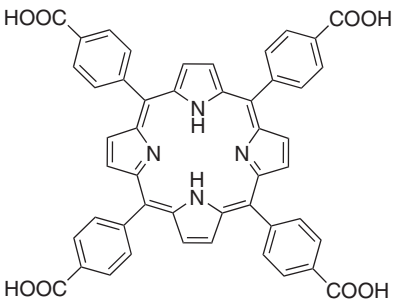

meso-tetra(4-carboxyphenyl)porphyrin (4)

Scheme 1. Structures of aniline (**1**), *para*- (**2**) and *meta*- (**3**) isomers of *meso*-tetrapyridylporphyrin and *meso*-4-tetra(carboxyphenyl)porphyrin) (**4**).

Table 1. Wave parameters (velocity and height) set for TWIM separation and transfer collision energy values for MS/MS experiments for each of the mass selected species used in this work

Compounds	*m/z*	Species	Wave velocity (m/s)	Wave height (V)	Transfer CE (V)
Aniline	94	$[M+H]^+$	300	16	25
tetra(3-pyridyl)porphyrin	619	$[M+H]^+$	180	30	70
tetra(4-pyridyl)porphyrin	619	$[M+H]^+$	180	30	70
tetra(3-pyridyl)porphyrin	310	$[M+2H]^{2+}$	300	25	40
tetra(4-pyridyl)porphyrin	310	$[M+2H]^{2+}$	300	25	40
tetra(4-carboxyphenyl)porphyrin	789	$[M-H]^-$ $[2M-2H]^{2-}$	300	30	40
tetra(4-carboxyphenyl)porphyrin	394	$[M-2H]^{2-}$	300	30	22

trap and transfer cells were operated at a pressure of 1.0×10^{-2} mbar of argon at 6 and 4 V, respectively. For MS/MS experiments using CID, trap parameters were kept the same, while transfer energy was increased to values optimized for each species (Table 1) depending on the fragment ion stability such that sufficient dissociation was achieved for structure determination. Experiments were acquired over the *m/z* range of 50 to 1000 and a mass resolving power of about 7000 at *m/z* 540.

Calculation of theoretical collision cross section

Structure optimization was performed using the density function theory basis sets B3LYP/6-311G(d,p) implemented in the Gaussian 3[19] molecular modeling software. Theoretical collision cross section (Ω) values were calculated using the open source software program MOBCAL[20] trajectory method.

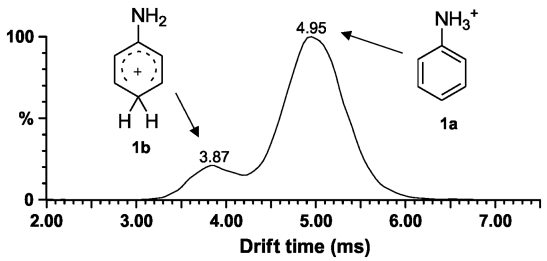

Figure 1. ESI(+)-TWIM-MS drift time plot showing the two protomers of the gaseous protonated species of *m/z* 94.07 sampled from an acidic methanolic solution (pH 4.0) of aniline.

RESULTS AND DISCUSSION

Figure 1 shows the TWIM-MS plot of mass selected protonated aniline (*m/z* 94.07) generated via ESI(+) from a methanolic and acidic solution of aniline. Note the two well-resolved peaks at 3.87 and 4.95 ms, and the relative intensity ratio of about 1:5. This quite gentle separation process, in which no substantial ion heating occurs thus avoiding any substantial collisional activation,[9] and the detection of the intact nearly undisturbed ion population, suggests that two gaseous protomers of aniline coexisted inside the TWIM cell at near room temperature, as observed by Karpas *et al.*[5] Methanolic solutions of aniline at different pHs (2.0, 4.0 and 7.0) were also investigated by TWIM-MS, and no changes in the 1:5 proportion were observed. Note that upon ESI(+), a drop of more than 4 pH units may occur due to the electrolytic oxidation of the solvent.[21] This constancy indicates 1:5 to be the intrinsic proportion of the two gaseous aniline protomers, but peak attribution is still missing as was the case in the Karpas experiment. [5]

To characterize the two separated protomers, post-TWIM CID was therefore performed in the transfer collision cell (Fig. 2). Interestingly, the slower, more abundant protomer (drift time of 4.95 ms) was found to dissociate nearly exclusively by NH_3 loss

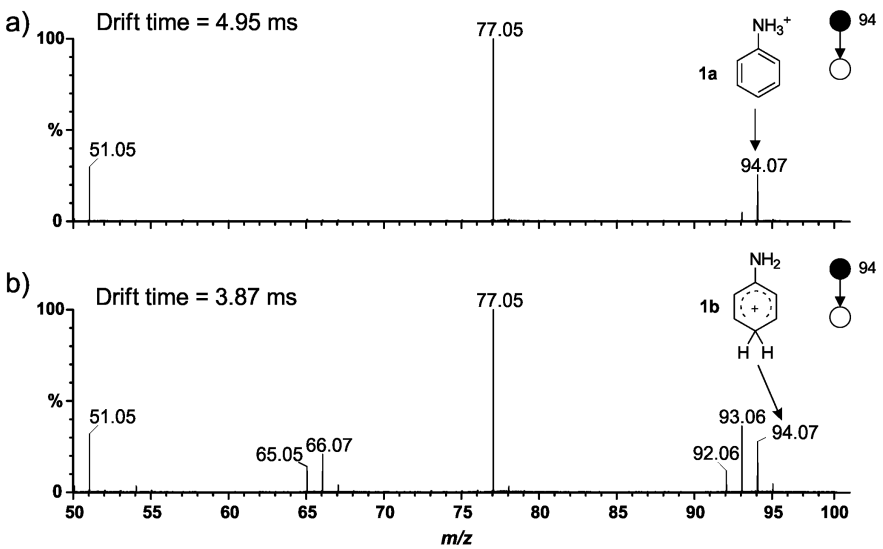

Figure 2. ESI(+)-TWIM-MS/MS of the two aniline protomers of *m/z* 94.07 with drift time equal to a) 4.95 ms and b) 3.87 ms.

Journal of MASS SPECTROMETRY

to give the phenyl cation of *m/z* 77.0516, which is known[8,22] to fragment further to the ion of *m/z* 51.0464 via acetylene loss (Fig. 2a). Note that this prompt and nearly exclusive NH_3 loss is consistent with the gaseous N-protonated species **1a** (Scheme 2). The less abundant protomer found at 3.87 ms also dissociates by NH_3 plus C_2H_2 loss (Fig. 2b), but other competitive pathways are observed indicating ring protonation (**1b**). Note that loss of NH_3 from **1b** seems to require **1b** → **1a** isomerization; hence, CID-induced isomerization may explain the contrasting results observed previously for aniline protomers sampled with different degrees of collision activation.[2–8]

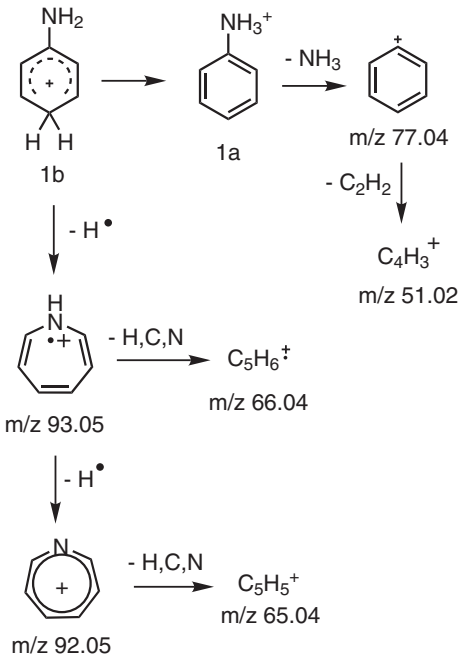

Scheme 2. Dissociation routes proposed for ring-protonated aniline (**1b**).

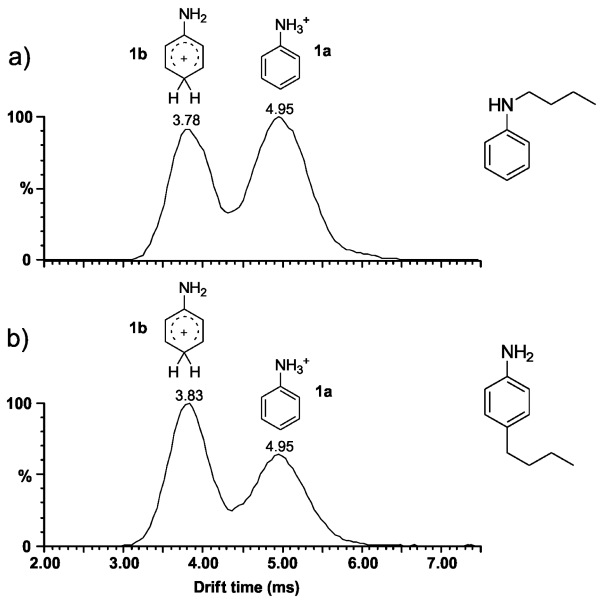

Figure 3. ESI(+)MS-TWIM-MS drift time plot for protomers of *m/z* 94.07 formed in the gas phase via pre-TWIM CID of mass-selected protonated a) N-butyl aniline and of b) *p*-butyl aniline.

Theoretical collision cross section (Ω) calculated for **1a** and **1b** (54.10 ± 4.20 Å^2 and 53.10 ± 4.20 Å^2, respectively) shows that protonation at different sites causes little change on the size or shape of this pair of protomers. Therefore, it seems that protomer separation by TWIM could be achieved mainly due to their contrasting charge distribution. Ions with uneven charge distribution and high polarity and/or high polarizability should form stronger proton bound heterodimers with the drift gas molecules with a lifetime long enough to survive over several mean free paths whereas ions with more delocalized charge are more largely free between collisions.[23] For this reason, the N-protonated aniline (at 4.95 ms), in which the positive charge is more localized in the NH_3^+ group, takes a longer time to travel through the TWIM cell and therefore can be separated from ring-protonated aniline (at 3.87 ms), in which the positive charge is delocalized in the benzene ring.

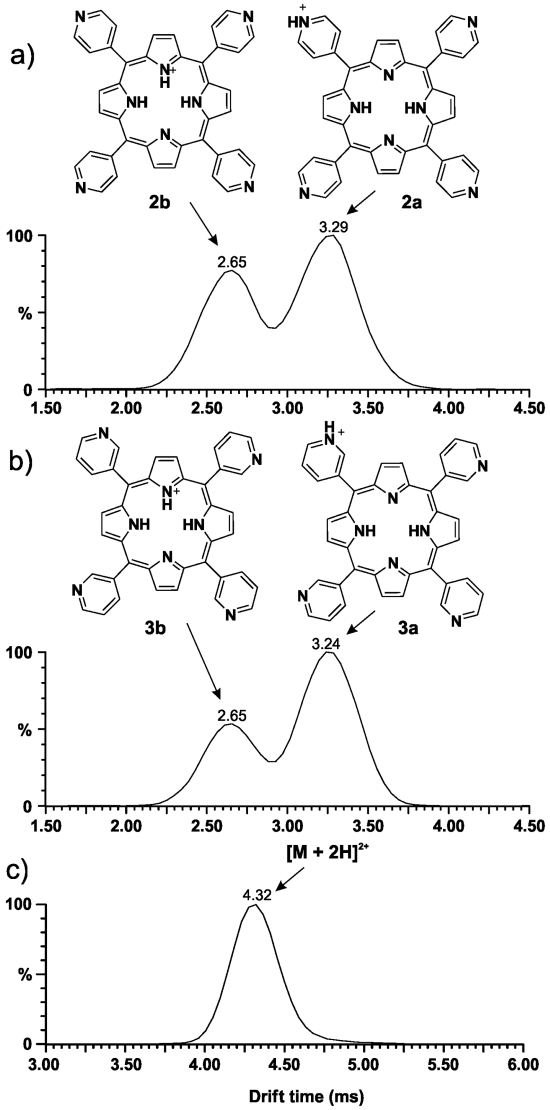

Figure 4. ESI(+)-TWIM-MS drift time plots of the singly charged protomers of *m/z* 619.24 from acidic methanolic solutions of a) *meso*-tetra(4-pyridyl)porphyrin (**2**) and b) *meso*-tetra(3-pyridyl)porphyrin (**3**) and c) of the doubly charged protomer of *m/z* 310.11 of *meso*-tetra (4-pyridyl)porphyrin (**2c**). Note that Fig. 4a–b and Fig. 4c plots were acquired with different wave parameters (Table 1), and therefore drift time values cannot be directly compared.

Interestingly, both N-butyl aniline and *p*-butyl aniline displayed a single protomer signal in TWIM-MS plot (not shown), and their CID chemistry was characterized by butane loss which is not elucidative for the assignment of the protonation site. However, such fragmentation process forms protonated aniline of *m/z* 94.07, which allowed us to investigate, via the unique pre-TWIM CID experiments offered by the Synapt design, the relative population of N- and ring-protonated protomers of aniline formed in the gas phase via CID of either protonated N-butyl aniline or *p*-butyl aniline (Fig. 3). Using such conditions, the population of the two aniline protomers differed considerably from that observed when the ions were sampled directly from acidic methanol solutions (Fig. 2). In both cases, the ring-protonated protomer **1b** was formed in much greater extent, such that its amount was even greater than the amount of N-protonated protomer **1a** when the protonated aniline was obtained from protonated *p*-butyl aniline by butene loss. The site of protonation in the parent molecule seems therefore to play a major role on the proportion of the nascent protomers of aniline, with N-alkylation but more pronouncedly ring-alkylation favouring ring protonation. Similar amounts of both protomers were generated from protonated N-butyl aniline. Clearly, the resulting pair of nascent protomers formed by CID with isolated species is not at the equilibrium condition. Accordingly, the intramolecular proton transfer process in the gas phase, required for the isomerization/interconversion of **1b** to **1a**, must be slow considering the time scale of TWIM-MS experiments.

Porphyrins, both from natural and synthetic sources, are molecules of great importance in many fields,[24] and pyridyl groups are particularly suitable as porphyrin substituents owing to their effective coordination properties.[25] ESI-MS[26] and ESI-TWIM-MS[17] have been used to characterize the isomers of ruthenated *meso*-pyridylporphyrins, but *meso*-tetrapyridylporphyrins (TPyP) also are interesting model systems due to the presence of multiple protonation sites. In fact, it is possible to add up to four protons to the peripheral pyridyl groups and two protons to the porphyrin ring allowing the formation of several protomers. The resulting protonated species is stabilized by solvation in aqueous or polar solvent solution, but electrostatic repulsion generally inhibits the formation of gaseous species protonated at multiple sites. Thus, TWIM-MS technique was used to resolve and characterize the species present in MS-selected mixtures of TPyP protomers. Methanolic solutions of the isomeric *meso*-tetra(4-pyridyl)porphyrin **(2)** and *meso*-tetra(3-pyridyl)porphyrin **(3)** were therefore separately analyzed. Surprisingly, two peaks were observed (Fig. 4a-b) for each of the monoprotonated $[M+H]^+$ isomers of *m/z* 619.24 suggesting the coexistence of two distinct protomers. This result indicates that protonation took place not only in the more basic peripheral pyridyl substituents, but also in the inner porphyrin ring generating an isomeric monoprotonated species. In contrast, the bis-protonated $[M+2H]^{2+}$ species of *m/z* 310.11 exhibited a well-defined, symmetrical single peak in the TWIM-MS drift time plot (Fig. 4c), suggesting the predominant formation of one doubly charged species among the three possible combinations: *cis*-pyridyl, *trans*-pyridyl and pyridyl-porphyrin ring. Probably, the 'vicinal' *cis*-pyridyl protonated species is the less stable species in gas phase, but it is rather difficult to decide which one is more stable among the remaining two doubly charged species.

These results contrast with those generally found in solution.[27] The monocationic ring-protonated species is not observed in solution because the bis-protonated porphyrin is preferentially formed after protonation of the peripheral pyridyl sites. This clearly shows that these sites, with more localized positive charges, are more strongly stabilized by solvation than the protonated porphyrin ring with much more delocalized positive charge inverting the protonation sequence found in the gas phase.

Figure 5 shows the TWIM-MS/MS for CID of the two separated 4-TPyP protomers **2a** and **2b**. The slower protomer **2a** (at 3.2ms)

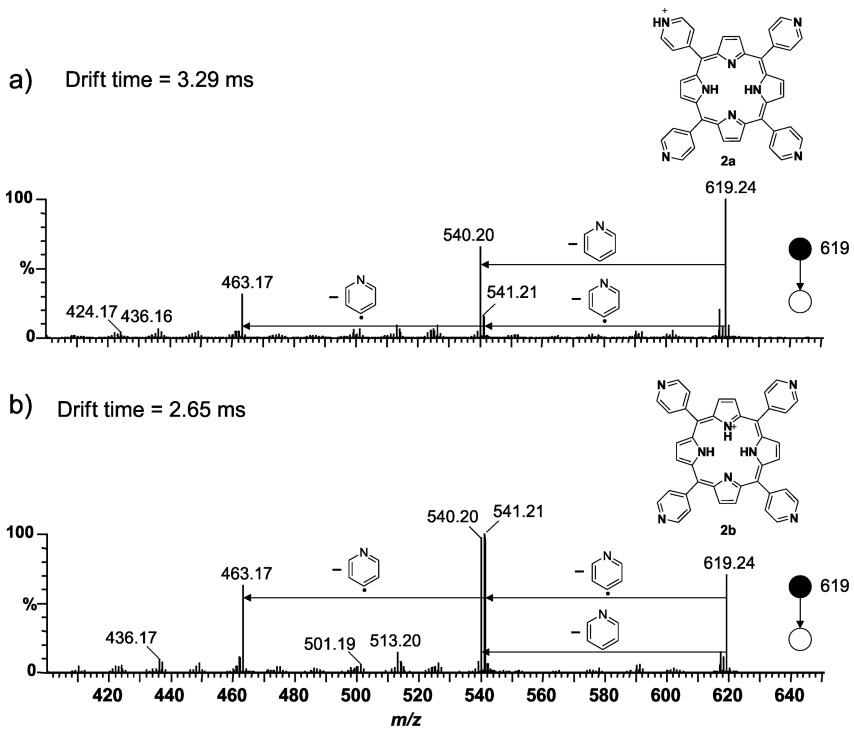

Figure 5. ESI(+)-TWIM-MS/MS of the two singly charged protomers of *m/z* 619.24 with drift time equal to a) 3.29 and b) 2.65 ms generated from acidic methanolic solution of *meso*-tetra(4-pyridyl)porphyrin (**2**).

loses preferentially neutral pyridine (*m/z* 540.2065) in the primary dissociation process, whereas the faster protomer **2b** dissociated forming neutral pyridine (*m/z* 540.2065) and a pyridyl radical (*m/z* 541.2140) to similar extents. The preferential loss of neutral pyridine is generally indicative of protonation at the pyridyl substituent, whereas loss of a pyridyl radical seems more consistent with the dissociation of a core protonated species. Therefore, the faster protomer **2b** (at 2.6 ms) was assigned to the inner N-porphyrinic ring-protonated species. The *meso*-tetra(3-pyridyl) porphyrin showed similar TWIM-MS/MS CID behaviour.

Again, the extent of charge delocalization seems to be useful to explain the elution (drift time) order of the pyridyl and porphyrin ring-protonated protomers of TPyP in CO_2 atmosphere. Charge density is highly localized in the pyridyl-protonated protomer **2a** (at 3.29 ms) which therefore should interact more strongly with CO_2 and is slowed down. The positive charge is, however, more delocalized in the core-protonated protomer **2b** (at 2.65 ms) thus explaining its faster elution. As for intrinsic basicity, the pyridyl group seems to be more basic and its proton affinity higher than the inner porphyrin ring N-pyrrolic sites, whereas *meta versus para* substitution seems to have little effect on those properties since

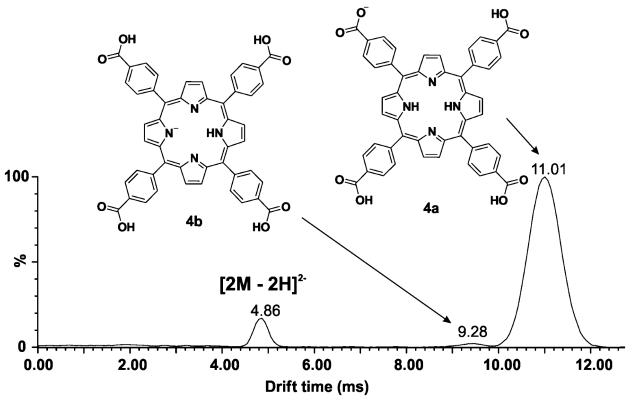

Figure 6. ESI(−)-TWIM-MS/MS drift time plot for the ions of *m/z* 789.28 generated from a basic methanolic *meso*-tetra(4-carboxyphenyl)porphyrin solution.

no significant change could be observed in the TWIM-MS/MS CID behavior as far as competition for protonation sites is considered.

The negatively charged 'de-protomers' generated by deprotonation of *meso*-tetra(4-carboxyphenyl)porphyrin (**4**) were also investigated by ESI(−)-TWIM-MS. Figure 6 shows the drift time plots for the selected ions of *m/z* 789.28. Note that three peaks were detected: one at 4.86 ms with an isotopomeric ion separation of 0.5 *m/z* revealing to be a doubly charged $[2M - 2H]^{2-}$ species; and two additional peaks at 9.28 and 11.01 ms corresponding to a couple of singly charged $[M - H]^-$ species, but the 11.01 ms species being much more abundant. Note that the doubly charged species are subjected to higher acceleration by the TWIM electric field and therefore display a much shorter drift time.

Post-TWIM CID was then performed for the two negatively charged protomers (Fig. 7). Interestingly, in a structurally diagnostic fashion,[28] the more abundant species at 11.01 ms promptly and near exclusively loses CO_2 (Fig. 7a), forming the ion of *m/z* 745.2836, whereas the less abundant species at 9.28 ms is much more stable under the same CID conditions (Fig. 7b). Prompt loss of CO_2 indicates deprotonation at the carboxylate group (**4a**) whereas resistance to dissociation is consistent with deprotonation at the porphyrin core (**4b**). Also, the significantly much lower basicity expected for the phenylcarboxylate substituent as compared with the deprotonated porphyrin ring species can account for the predominant deprotonation of the carboxylic acid group in **4**.

According to the above discussed results, the monoanionic species **4a** formed by deprotonation of a peripheral carboxylate group is observed at 11.0 ms in the drift time plot, been slower than **4b** (9.3 ms), due likely to more localized negative charge distribution and hence stronger interaction with the drift gas molecules (CO_2).

As Fig. 8a shows, TWIM-MS of the doubly deprotonated *meso*-tetra(4-carboxyphenyl)porphyrin **4** of *m/z* 394.1, viz. $[M - 2H]^{2-}$ species, shows a quite sharp and symmetrical single peak indicative of formation of a single doubly charged species **4c**. Its post-TWIM CID data (Fig. 8b) shows an interesting chemistry with two consecutive losses of CO_2, that is CO_2^- (*m/z* 700.2799) and then neutral CO_2 (*m/z* 744.2723) therefore indicating deprotonation at two carboxylic acid groups, probably in *trans* position for maximum charge separation. In this case, the energy difference

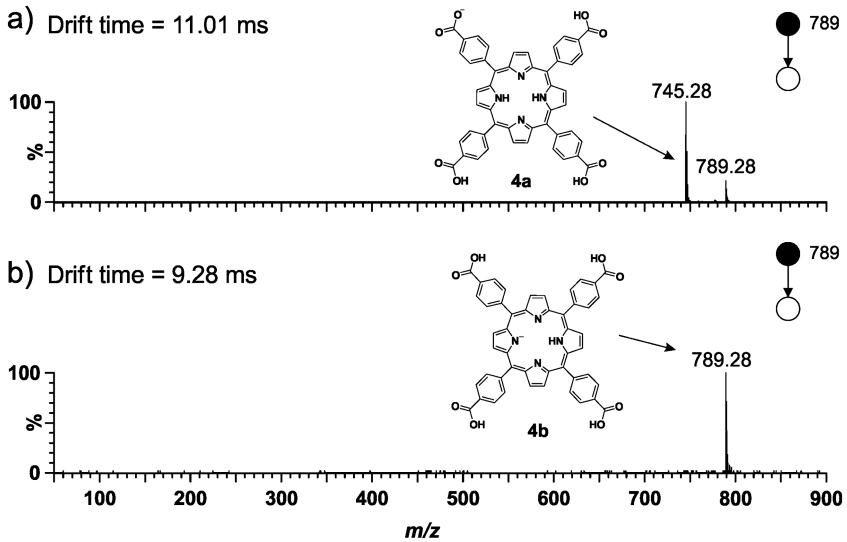

Figure 7. ESI(−)-TWIM-MS/MS for CID of the two singly charged 'de-protomers' of *m/z* 789.28 with drift time equal to a) 11.01 ms and b) 9.28 ms generated from a basic methanolic solution of *meso*-tetra(4-carboxyphenyl)porphyrin (**4**).

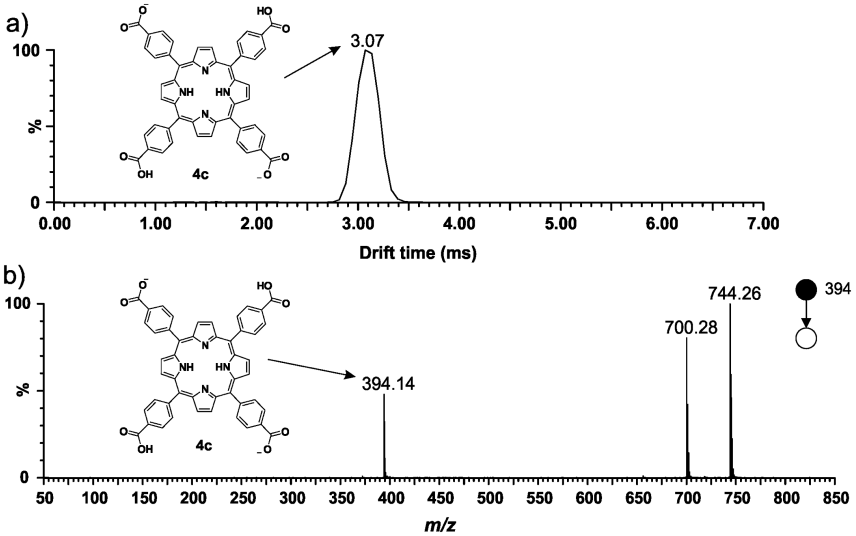

Figure 8. a) ESI(−)-TWIM-MS drift time plot and b) ESI(−)-TWIM-MS/MS for post-TWIM CID of the doubly deprotonated *meso*-tetra(4-carboxyphenyl) porphyrin of *m/z* 394.14.

for formation of the deprotonated porphyrin ring is much higher than for the deprotonation of a second carboxylic acid group, thus generating the *trans* dianionic species **4c**. Interestingly, there is no indication of the co-existance of the *trans*- and *cis*-carboxylate species, which points to high enough electrostatic repulsion ensuring only the formation of the *trans* protomer **4c**.

CONCLUSION

Singly or doubly charged protomers of aniline and/or several porphyrins have been formed, separated and characterized using TWIM-MS and TWIM-MS/MS experiments employing pre-TWIM and post-TWIM CID. Although these isomers display similar sizes and shapes, and the same charges, protonation or deprotonation in different sites causes substantial differences in charge distributions that seem to be the major effect promoting proper separation in the TWIM cell using the polarizable CO_2 as the drift gas. Proton bound heterodimers with CO_2 of contrasting strengths and lifetimes are likely formed, hence ensuring their proper resolution. Post-TWIM CID enabled protomers to be characterized via structurally diagnostic CID, and such characterization was for the first time done for aniline protomers. Protomer ratios for aniline sampled from equilibrium in solution or formed in isolated forms in non-equilibrium conditions in the gas phase via pre-TWIM CID were also shown via TWIM-MS to vary substantially. Protonated aniline sampled from solution equilibrium was found to be consistent with a mixture of two protomers, the *N*-protonated and ring-protonated species, in ca. 5:1 ratio whereas these two isomers were produced in different relative amounts from gas phase CID of specific precursor molecules at non-equilibrium conditions. For the porphyrins, the formation of unusual ring-protonated and deprotonated porphyrin species was observed in the gas phase. TWIM-MS(/MS) with pre- or post-TWIM CID has been shown therefore to offer a powerful structural tool enabling the investigation of protomers and 'de-protomers'; hence revealing intrinsic acidities and basicities at competing sites for poly or multifunctional molecules both from solution or gas phase processes.

Acknowledgements

We thank FAPESP, CNPq, FINEP and CAPES for financial support.

REFERENCES

[1] (a) A. Largo, C. Barrientos. Theoretical studies of possible processes for the interstellar production of phosphorus compounds. Reaction of P^+ with HCN and protonation of CNP compounds. *J. Phys. Chem.* **1991**, *95*, 9864. (b) K. A. Cox, S. J. Gaskell, M. Morris, A. Whiting. Role of the site of protonation in the low-energy decompositions of gas-phase peptide ions. *J. Am. Soc. Mass Spectrorn.* **1996**, *7*, 522. (c) J. Graton, M. Berthelot, J.-F. Gal, S. Girard, C. Laurence, J. Lebreton, J.-Y. Le Questel, P.-C. Maria, P. Naus. Site of protonation of nicotine and nornicotine in the gas phase: pyridine or pyrrolidine nitrogen? *J. Am. Chem. Soc.* **2002**, *124*, 10552. (d) O. Dopfer, N. Solca, J. Lemaire, P. Maitre, M.-E. Crestoni, S. Fornarini. Protonation sites of isolated fluorobenzene revealed by ir spectroscopy in the fingerprint range. *J. Phys. Chem. A* **2005**, *109*, 7881.

[2] S. K. Pollack, J. L. Devlin, K. D. Summerhays, R. W. Taft, W. J. Hehre. The site of protonation in aniline. *J. Am. Chem. Soc.* **1977**, *99*, 4583.

[3] Y. K. Lau, P. Kebarle. Substituent effects on intrinsic basicity of benzene - proton affinities of substituted benzenes. *J. Am. Chem. Soc.* **1976**, *98*, 7452.

[4] (a) K. V. Wood, D. J. Burinsky, D. Cameron, R. G. Cooks. Site of gas-phase cation attachment - protonation, methylation, and ethylation of aniline, phenol, and thiophenol. *J. Org. Chem.* **1983**, *48*, 5236. (b) S. J. Pachuta, I. Isern-Flecha, R. G. Cooks. Charge stripping and the site of cationization of substituted aromatic-compounds. *Org. Mass Spectrom.* **1986**, *21*, 1.

[5] Z. Karpas, Z. Berant, R. M. Stimac. An ion mobility spectrometry/mass spectrometry (IMS/MS) study of the site of protonation in anilines. *Struct.Chem.* **1990**, *1*, 201.

[6] R. L. Smith, L. J. Chyall, B. J. Beasley, H. I. Kenttamaa. The site of protonation of aniline. *J. Am. Chem. Soc.* **1995**, *117*, 7971.

[7] N. Russo, M. Toscano, A. Grand, T. Mineva. Proton affinity and protonation sites of aniline. Energetic behavior and density functional reactivity indices. *J. Phys. Chem. A* **2000**, *104*, 4017.

[8] R. Flammang, N. Dechamps, L. Pascal, Y. Van Haverbeke, P. Berbaux, P. C. Nam, M. T. Nguyen. Ring *versus* nitrogen protonation of anilines. *Org. Chem. Lett.* **2004**, *1*, 23.

[9] H. Borsdorf, G. Eiceman. Ion mobility spectrometry: Principles and applications. *Appl. Spectros. Rev.* **2006**, *41*, 323.

[10] A. B. Kanu, P. Dwivedi, M. Tam, L. Matz, H. H. Hill. Ion mobility-mass spectrometry. *J. Mass Spectrom.* **2008**, *43*, 1–22. (b) S. Armenta, M. Alcala, M. Blanco. A review of recent, unconventional applications of ion mobility spectrometry (IMS). *Anal. Chim. Acta* **2011**, *703*, 114.

[11] (a) P. Dwivedi, C. Wu, L. M. Matz, B. H. Clowers, W. F. Siems, H. H. Hill. Gas-phase chiral separations by ion mobility spectrometry. *Anal. Chem.* **2006**, *78*, 8200. (b) M. Benassi, Y. E. Corilo, D. Uria, R. Augusti, M. N. Eberlin. Recognition and resolution of isomeric alkyl anilines by mass spectrometry. *J. Am. Soc. Mass Spectrom.* **2009**, *20*, 269. (c) M. Zhu, B. Bendiak, B. Clowers, H. H. Hill. Ion mobility-mass spectrometry analysis of isomeric carbohydrate precursor ions. *Anal. Bioanal. Chem.* **2009**, *394*, 1853.

[12] S. Trimpin, D. E. Clemmer. Ion mobility spectrometry/mass spectrometry snapshots for assessing the molecular compositions of complex polymeric systems. *Anal. Chem.* **2008**, *80*, 9073.

[13] F. A. Fernandez-Lima, C. Becker, A. M. McKenna, R. P. Rodgers, A. G. Marshall, D. H. Russell. Petroleum crude oil characterization by IMS-MS and FTICR MS. *Anal. Chem.* **2009**, *81*, 9941.

[14] E. R. Brocker, S. E. Anderson, B. H. Northrop, P. J. Stang, M. Bowers. Structures of metallosupramolecular coordination assemblies can be obtained by ion mobility spectrometry-mass spectrometry. *J. Am. Chem. Soc.* **2010**, *132*, 13486.

[15] (a) G. Von Helden, T. Wyttenbach, M. T. Bowers. Conformation of macromolecules in the gas-phase - use of matrix-assisted laser-desorption methods in ion chromatography. *Science* **1995**, *267*, 1483. (b) D. E. Clemmer, R. R. Hudgins, M. F. Jarrold. Naked protein conformations - cytochrome-c in the gas-phase. *J. Am. Chem. Soc.* **1995**, *117*, 10141. (c) T.-Y. Kim, S. J. Valentine, D. E. Clemmer, J. P. Reilly. Gas-phase conformation-specific photofragmentation of proline-containing peptide ions. *J. Am. Soc. Mass Spectrom.* **2010**, *21*, 1455.

[16] (a) K. Giles, S. D. Pringle, K. R. Worthington, D. Little, J. L. Wildgoose, R. H. Bateman. Applications of a travelling wave-based radio-frequencyonly stacked ring ion guide. *Rapid Commun. Mass Spectrom.* **2004**, *18*, 2401. (b) S. D. Pringle, K. Giles, J. L. Wildgoose, J. P. Williams, S. E. Slade, K. Thalassinos, R. H. Bateman, M. T. Bowers, J. J. Scrivens. An investigation of the mobility separation of some peptide and protein ions using a new hybrid quadrupole/travelling wave IMS/oa-ToF instrument. *Int. J. Mass Spectrom.* **2007**, *261*, 1. (c) A. A. Shvartsburg, R. D. Smith. Fundamentals of traveling wave ion mobility spectrometry. *Anal. Chem.* **2008**, *80*, 9689.

[17] P. M. Lalli, B. A. Iglesias, D. K. Deda, H. E. Toma, G. F. Sa, R. J. Daroda, K. Araki, M. N. Eberlin. Resolution of isomeric multi-ruthenated porphyrins by travelling wave ion mobility mass spectrometry. *Rapid Commun. Mass Spectrom.* **2012**, *26*, 263.

[18] (a) L. W. Beegle, I. Kanik, L. Matz, H. H. Hill. Effects of drift-gas polarizability on glycine peptides in ion mobility spectrometry. *Int. J. Mass Spectrom.* **2002**, *216*, 257. (b) Z. Karpas, Z. Berant. Effect of drift gas on mobility of ions. *J. Phys. Chem.* **1989**, *93*, 3021.

[19] M. J. Frisch, G. W. Trucks, H. B. Schlegel, G. E. Scuseria, M. A. Robb, J. R. Cheeseman, J. A. Montgomery, Jr., T. Vreven, K. N. Kudin, J. C. Burant, J. M. Millam, S. S. Iyengar, J. Tomasi, V. Barone, B. Mennucci, M. Cossi, G. Scalmani, N. Rega, G. A. Petersson, H. Nakatsuji, M. Hada, M. Ehara, K. Toyota, R. Fukuda, J. Hasegawa, M. Ishida, T. Nakajima, Y. Honda, O. Kitao, H. Nakai, M. Klene, X. Li, J. E. Knox, H. P. Hratchian, J. B. Cross, V. Bakken, C. Adamo, J. Jaramillo, R. Gomperts, R. E. Stratmann, O. Yazyev, A. J. Austin, R. Cammi, C. Pomelli, J. W. Ochterski, P. Y. Ayala, K. Morokuma, G. A. Voth, P. Salvador, J. J. Dannenberg, V. G. Zakrzewski, S. Dapprich, A. D. Daniels, M. C. Strain, O. Farkas, D. K. Malick, A. D. Rabuck, K. Raghavachari, J. B. Foresman, J. V. Ortiz, Q. Cui, A. G. Baboul, S. Clifford, J. Cioslowski, B. B. Stefanov, G. Liu, A. Liashenko, P. Piskorz, I. Komaromi, R. L. Martin, D. J. Fox, T. Keith, M. A. Al-Laham, C. Y. Peng, A. Nanayakkara, M. Challacombe, P. M. W. Gill, B. Johnson, W. Chen, M. W. Wong, C. Gonzalez, J. A. Pople. *Gaussian 03, Revision B.05*. Gaussian, Inc.: Wallingford, CT, **2004**.

[20] (a) M. F. Mesleh, J. M. Hunter, A. A. Shvartsburg, G. C. Schatz, M. F. Jarrold. Structural information from ion mobility measurements: Effects of the long-range potential. *J. Phys. Chem.* **1996**, *100*, 16082. (b) M. F. Jarrold. website. http://www.indiana.edu/~nano/software.html

[21] G. J. Van Berkel, F. Zhou, J. T. Aronson. Changes in bulk solution pH caused by the inherent controlled-current electrolytic process of an electrospray ion source. *Int. J. Mass Spectrom.* **1997**, *162*, 55.

[22] A. V. Robertson, M. Marx, C. Djerassi. Question of ring expansion in electron impact-induced fragmentation of aromatic amines. *Chem. Commun.* **1968**, *206*, 414.

[23] Z. Karpas, M. J. Cohen, R. M. Stimac, R. F. Wernlund. On the effects of structure and charge-distribution on the mobility of ions. *Int. J. Mass Spectrom.Ion Process.* **1986**, *74*, 153.

[24] (a) K. M. Kadish, K. M. Smith, R. Guilard. *The Porphyrin Handbook*, Vol. *1–20*. Academic Press: San Diego, **2000–2003**. (b) J. Setsune. Palladium chemistry in recent porphyrin research. *J. Porph. Phthalocyan.* **2004**, *8*, 93.

[25] R. C. Rocha, K. Araki, H. E. Toma. Intervalence transfer properties of the binuclear mu-benzotriazolate- and mu-benzimidazolate-bis {ruthenium(II)/(III)-edta} complexes. *Inorg. Chim. Acta* **1999**, *285*, 197.

[26] (a) D. M. Tomazela, F. C. Gozzo, I. Mayer, F. M. Engelmann, K. Araki, H. E. Toma, M. N. Eberlin. Electrospray mass and tandem mass spectrometry of homologous and isomeric singly, doubly, triply and quadruply charged cationic ruthenated *meso*-(phenyl)(m)-(meta- and para-pyridyl)(n) (m + n = 4) macrocyclic porphyrin complexes. *J. Mass Spectrom.* **2004**, *39*, 1161. (b) S. H. Toma, A. D. P. Alexiou, H. E. Toma, M. N. Eberlin, K. Araki. Can mass dissociation patterns of transition-metal complexes be predicted from electrochemical data? *J. Mass Spectrom.* **2009**, *44*, 361.

[27] (a) H. Winnischofer, F. M. Engelmann, H. E. Toma, K. Araki. Acid–base and spectroscopic properties of a novel supramolecular porphyrin bonded to four pentacyanoferrate(II) groups. *Inorg. Chim. Acta* **2002**, *338*, 27. (b) P. Stepanek, V. Andrushchenko, K. Ruud, P. Bour. Porphyrin protonation studied by magnetic circular dichroism. *J. Phys. Chem. A* **2012**, *116*, 778.

[28] M. Eberlin. Structurally diagnostic ion/molecule reactions: class and functional-group identification by mass spectrometry. *J. Mass Spectrom.* **2006**, *41*, 141.

